Distribution Agreement

In presenting this thesis as a partial fulfillment of the requirements for a degree from Emory University, I hereby grant to Emory University and its agents the non-exclusive license to archive, make accessible, and display my thesis in whole or in part in all forms of media, now or hereafter now, including display on the World Wide Web. I understand that I may select some access restrictions as part of the online submission of this thesis. I retain all ownership rights to the copyright of the thesis. I also retain the right to use in future works (such as articles or books) all or part of this thesis.

Maya Shah April 1, 2021

Novel Opsins and Oxygen Induced Retinopathy

by

Maya Shah

Michael Iuvone, PhD
Adviser

Neuroscience and Behavioral Biology

Michael Iuvone, PhD

Adviser

LaTonia Taliaferro-Smith, PhD

Committee Member

Donald Stein, PhD

Committee Member

Daniel Dilks, PhD

Committee Member

2021

Novel Opsins and Oxygen Induced Retinopathy

By

Maya Shah

Michael Iuvone, PhD

Adviser

An abstract of
a thesis submitted to the Faculty of Emory College of Arts and Sciences
of Emory University in partial fulfillment
of the requirements of the degree of
Bachelor of Science with Honors

Neuroscience and Behavioral Biology

2021

Abstract

Novel Opsins and Oxygen Induced Retinopathy
By Maya Shah

Background: Retinopathy of prematurity (ROP) is a major complication of preterm birth that can lead to different degrees of vision impairment. The ROP spectrum ranges from mild forms that may resolve spontaneously or advanced stage diagnoses indicative of retinal detachment and subsequent blindness. Evidence suggests that light activation of OPN4 and OPN5 may be used to reduce neovascularization in a mouse model of ROP. This study serves as a launching point for an investigation of novels opsins and OIR.

Methods: Studying oxygen-induced retinopathy (OIR) in mice has been a valuable mode of investigating the pathology of ROP and treatment options in a pre-clinical *in vivo* model. Retinopathy was induced by exposing mice to 75% oxygen from postnatal day 7 (P7) to P12 in wild type C57BL/6J mice and *Opn4* and *Opn5* mutant mice. Wild type C57BL/6J mice were sacrificed at P17 and the *Opn4* line was sacrificed at P12. To quantify vasculature, a novel technique for 3D analysis was developed using Imaris software.

Results: Retinal vasculature of OIR mice occupied a smaller area, were less volumetric, and exhibited fewer branch points than control mice at P17. Wild type C57BL/6J mice did not show quantifiable evidence of neovascularization in the periphery of the retina. Preliminary images from the P12 *Opn4* line serve as visual evidence of an avascular zone at the center of the retina.

Conclusion: The results suggest that some degree of retinopathy was induced in wild type C57BL/6J mice and the *Opn4* line. Continued experiments on wildtype and genetically modified mice that quantify OIR at different points of retinal development is imperative before applying light therapy as a treatment option.

Novel Opsins and Oxygen Induced Retinopathy

By

Maya Shah

Michael Iuvone, PhD

Adviser

A thesis submitted to the Faculty of Emory College of Arts and Sciences
of Emory University in partial fulfillment
of the requirements of the degree of
Bachelor of Science with Honors

Neuroscience and Behavioral Biology

2021

Acknowledgements

I would like to thank Dr. Michael Iuvone for his endless support and guidance throughout my experience in his laboratory. I would also like to thank Jessica Hamm and Micah Chrenek for their continued assistance and time spent on helping me complete my thesis. Finally, I would like to thank my family and friends for their words of encouragement and support through this research experience.

Table of Contents

Abstract

Background: Retinopathy of prematurity (ROP) is a major complication of preterm birth that can lead to different degrees of vision impairment. The ROP spectrum ranges from mild forms that may resolve spontaneously or advanced stage diagnoses indicative of retinal detachment and subsequent blindness. Evidence suggests that light activation of OPN4 and OPN5 may be used to reduce neovascularization in a mouse model of ROP. This study serves as a launching point for an investigation of novels opsins and OIR.

Methods: Studying oxygen-induced retinopathy (OIR) in mice has been a valuable mode of investigating the pathology of ROP and treatment options in a pre-clinical *in vivo* model. Retinopathy was induced by exposing mice to 75% oxygen from postnatal day 7 (P7) to P12 in wild type C57BL/6J mice and *Opn4* and *Opn5* mutant mice. Wild type C57BL/6J mice were sacrificed at P17 and the *Opn4* line was sacrificed at P12. To quantify vasculature, a novel technique for 3D analysis was developed using Imaris software.

Results: Retinal vasculature of OIR mice occupied a smaller area, were less volumetric, and exhibited fewer branch points than control mice at P17. Wild type C57BL/6J mice did not show quantifiable evidence of neovascularization in the periphery of the retina. Preliminary images from the P12 *Opn4* line serve as visual evidence of an avascular zone at the center of the retina.

Conclusion: The results suggest that some degree of retinopathy was induced in wild type C57BL/6J mice and the *Opn4* line. Continued experiments on wildtype and genetically modified mice that quantify OIR at different points of retinal development is imperative before applying light therapy as a treatment option.

1. Introduction

1.1 Background and Overview of ROP

Retinopathy of prematurity is an eye disease that occurs in premature infants as a result of abnormal vessel growth in the retina (Owen et al., 2017). It is estimated that 30% of infants born preterm will develop retinopathy of prematurity (ROP) (Quinn et al., 2018). Retinopathy of prematurity remains a leading cause of blindness in developed and developing countries (Arnesen et al., 2016). In the United States, 400-600 infants become blind from ROP each year (Owen et al., 2017).

In 1942, Terry first identified retinopathy of prematurity through investigating numerous case reports and characterized it as a bilateral fibroplasia (Terry, 1942). The disease was distinguishable by the fibroblastic sheath formed behind the lens and the complete retinal detachment. As cases were primarily reported in premature infants, it was correctly suspected that prematurity was a predisposing condition. The severity of retinopathy is inversely related to gestational age and weight (Smith, 2003). Hyperoxic conditions were used to compensate for incomplete lung development and it was observed that retinal vascularization halted as a result. Therefore, monitoring oxygen levels became a critical aspect of the development of retinopathy.

Early on, improper oxygen administration and lack of proper neonatal care contributed to increased diagnosis of retinopathy (Carlo and Higgins, 2010). Clinical trials in the 1950s found that restricting the oxygen concentration reduced the relative risk of retinopathy by 50%, but increased the rate of mortality (Askie et al., 2009). To better understand the association between oxygen concentration and retinopathy, Smith developed a method of inducing

retinopathy in a mouse model via oxygen chambers (Smith, 1994). With a reliable and replicable model for studying the disease, recent years have seen greater attention on ROP.

Despite advancements in neonatology, ROP remains a serious problem. Current treatments for ROP include laser treatment and cryotherapy. Both treatments resolve the retinopathy by destroying the peripheral areas of the retina with neovascularization. However, the treatment is only available to infants in advanced stages and the invasiveness of the procedure can result in damage of peripheral vision. A preventative therapy for ROP is necessary to avoid severe complications that can manifest.

1.2 Pathology of ROP

Retinal vascular development commences during the first 16 weeks of gestation through vasculogenesis. Ideally, retinal development is completed while the fetus is still in the uterus in a relatively hypoxic environment (Smith, 2003). When born premature, infants have incompletely developed retinal vasculature consisting of a peripheral avascular zone. The immaturity in retinal development predisposes the retina to complications. ROP is a two-phase disease in which incomplete retinal vascular development after premature birth is compounded with hypoxia to release factors that stimulate abnormal blood vessel growth (Sapieha et al., 2010). During the first phase of ROP, the comparatively high oxygen concentrations that the infant is exposed to ceases the process of retinal vasculogenesis. High oxygen concentrations are needed due incomplete lung development. When removed from the high oxygen environment, the retina becomes hypoxic and precipitates the release of angiogenic compounds that allow for aberrant growth of retinal blood vessels. The neovascularization generates fibrous scar tissue and subsequent retinal detachment.

1.3 Oxygen-Induced Retinopathy (OIR) as a Model

In 1994, Smith developed a method of mirroring the effects of hypoxic conditions on retinal development in mice (Smith et al., 1994). Unlike humans, mice continue to develop their retinal vasculature postnatally. Human infants born at term have fully mature retinas, while mice have immature retinal development that mimics what is seen in premature human infants (Kim et al., 2016). The mouse retina develops shortly after gestation in a predictable, organized, and time-regulated manner. The temporal and spatial patterns of vascular plexuses in the retina are highly reproducible and easily manipulated (Dorrell and Friedlander, 2006). This makes the mouse an ideal and inducible model of ROP.

The method developed by Smith et al. (1994) is the current standard for OIR studies in mice. The model involves two stages. Newborn mice are exposed to 75% oxygen concentration from postnatal day 7 (P7) to P12. During this developmental period, the retinal vasculature is immature and susceptible to hyperoxia damage. The high oxygen concentration targets the capillaries adjacent to arteries in the center of the retina, leaving behind a capillary free zone. This capillary obliteration is likely due to the toxic effect of high oxygen on endothelial cells (Beauchamp et al., 2004). Hyperoxic conditions do not have substantial effect on the development of larger more prominent arteries that extend from the center to the periphery (Scott and Fruttiger, 2010). Using mice any older than P7 would essentially be ineffective because the maturation of arteries and veins in this region has already occurred. The second stage is initiated when the mice are moved from hyperoxic conditions to normoxia or room air. The retina becomes hypoxic and this triggers a vascular repair response, resulting in the

formation of neovascular tufts in the periphery of the retina. Essentially, the first phase results in vaso-obliteration in the center of the retina while the second phase causes neovascularization and tuft formation in the periphery. Although OIR is the model of choice, it is important to note that there are notable differences between OIR and ROP. ROP has many other factors contributing to the disease pathology, whereas in OIR models oxidative stress is the major pathological abnormality (Scott and Fruttiger, 2010).

1.4 Quantification of Vasculature

Investigating novel techniques for quantifying the health and development of retinal vascular networks is important experimentally and clinically. With a space for various approaches to be developed, quantification of retinal vasculature had been difficult to standardize among researchers. This has made it challenging to directly compare retinal studies. The gold standard approach to quantification involves manually counting the nuclei of new vessels. Each retina could take anywhere between 20 to 40 minutes to analyze and requires the same user to analyze each image. The model proposed by Smith is often used in conjunction with a technique developed by researchers to quantify vaso-obliteration (Connor et al., 2009). Adobe Photoshop is employed for semi automated analysis. The Polygonal Lasso tool is used to trace the entire vascular retina and subtracted from the entire selection. This allows the user to measure the avascular zone. The action can be reversed so that the avascular zone is selected and subtracted, leaving the vascular zone quantified. This technique still requires manual tracing and is susceptible to user variability.

ImageJ (also known as Fiji) offers a similar function to Adobe Photoshop, but with less manual tracing. In this method, the background is subtracted from a tracing of the perimeter of the whole flatmount instead of the tufts and clusters of vascularization. This makes it possible to calculate the corrected cellular fluorescence. Within ImageJ, several macros for specifically analyzing retinal vasculature have also been developed. For example, The SWIFT_NV macro can be used to quantify vasculature with little user-interference (Stahl et al., 2009). However, ImageJ and Adobe Photoshop both analyze the image in 2D with no visualization of the 3D structure. With retinal vasculature developing in highly orchestrated spatiotemporal sequence, a closer examination of the 3D structure could reveal novel properties of the retina.

The Imaris Bitplane software with the Imaris for Neuroscientists package offers 3D/4D visualization via the filament tracer tool. This software enables automatic detection of filamentous structures for volume rendering, cross sectional slicing, and clipping planes. Generally, Imaris has an interface that is more compatible with filamentous detection and requires no tracing.

1.5 Oxygen Therapy

With much evidence pointing in the direction of oxygen therapy, one study conducted a meta-analysis to determine the association between ROP and high and low oxygen saturation (Chen et al., 2010). Low oxygen saturation (70-96%) in the first few weeks following birth was associated with a 52% reduction in developing severe ROP in human infants. However, additional research offers conflicting results. One clinical trial assessed rates of ROP in 1,187 preterm with either 85-89% or 91-95% oxygen saturation, assessed by pulse oximetry (BOOST II

et al., 2013). This study was halted prematurely due to the increased risk of mortality in infants in the 85%-89% group, but preliminary data also revealed that infants in this group had a reduced incidence of ROP. A major limitation in applying this technique to clinical practices is that low oxygen saturation significantly increases the chances of mortality (Chang, 2011). The immature lungs of a preterm infant cannot sustain adequate oxygen levels on their own and, thus, require high concentrations of oxygen. Although low oxygen saturation can reduce the severity of ROP, it often leads to failure in other parts of the body. Despite evidence of reduced incidence of ROP, these studies do not provide any guidance on how to reduce the risk of both ROP and mortality using oxygen therapy.

1.6 Anti-Angiogenesis Therapy

The abnormal growth of retinal vasculature is driven by the release of angiogenic compounds. Another perspective in treating ROP focuses on inhibiting the release of angiogenic compounds. Vascular endothelial growth factor (VEGF) is required for retinal vascularization and development in preterm infants. VEGF-mediated angiogenesis is promoted by hypoxia-dependent signaling. Intravitreal injections of anti-VEGF antibodies were shown to decrease heightened VEGF conditions in the ocular fluid (Wang, 2016). Although this was effective in delaying the regression of ROP, reduced VEGF conditions persisted for 2 months following treatment. The reduction in systemic VEGF following intravitreal injection has been associated with abnormal body growth and organ development in preterm infants. Additionally, clinical translation of anti-VEGF studies in treating severe ROP lead to peripheral avascular retina (AHA), recurrent intravitreal neovascularization (IVNV), and late retinal detachment

1-year post-treatment (McCloskey et al., 2013). This suggests major limitations of anti-VEGF therapy, but research persists in investigating the effect of dosage, optimal treatment window, and long-term effects of administering anti-VEGF.

Other studies have looked at specific vascular endothelial growth factors, specifically VEGF-A. The decline in visual performance has been associated with dopamine deficiency in hypoxic retinopathies. Dopaminergic amacrine cells (DACs) within the inner nuclear layer (INL) perceive changes in oxygen levels and adjust VEGF-A levels in response (Eglen et al., 2003). Instead of controlling angiogenic release in the neuroretina, one study evaluated the retinal response to VEGF-TRAP (Aflibercept) on DACs (Arias et al., 2019). This treatment led to a significant reduction in neovascular tuft formation and cell proliferation in OIR retinas. However, discontinuation of the treatment results in a re-emergence of vascular aberrations. The correct dosage and treatment plan has to be determined to translate this into clinical studies. Along with this, the concern that intravitreal anti-angiogenic agents can produce systemic issues in preterm infants is ever-present. Some research indicates that anti-angiogenic compounds used as an intervention for cancers and ocular diseases can even lead to cutaneous side-effects and wound healing complications (Bodnar, 2014).

1.7 Melanopsin and Light

With anti-angiogenesis and oxygen therapies leading to complications, ROP requires a treatment that reduces retinopathy without adverse side effects. In 2010, Johnson et al. (2010), found that neonatal mice are light-responsive and show changes in neural connectivity upon differential lighting conditions. This prompted an investigation into the ability of light to reduce or prevent ROP. Some studies have found that increased average day length (ADL) is associated

with a reduced risk of developing severe ROP. In one study, Yang et al. (2013) found that each additional hour of ADL decreased the risk of severe ROP by 28%. Although these results could be confounded by seasonal variation in light exposure during gestation, it reveals the benefit of light in mitigating the risk of ROP. These findings suggest that prophylactic light treatment during late gestation can reduce the potential development of ROP.

The findings regarding ADL are consistent with experiments demonstrating that external light reaching the fetus can activate melanopsin retinal ganglion cells in mice (Rao et al., 2013). Researchers found that dark rearing of dams and pups a week postpartum had delayed the regression of hyaloid vessels. Since hyaloid regression and retinal angiogenesis occur at the same time in mice, this suggests the ability of light to influence retinal vascular development. The light is activating specific light-sensitive cells that resultantly promote hyaloid regression. To evaluate candidates for this, the intrinsically-photosensitive melanopsin retinal ganglion cells was chosen because of the vascular abnormalities of mice lacking retinal ganglion cells. Melanopsin is encoded by the *Opn4* gene. Melanopsin-expressing retinal ganglion cells are present in the early days of both human and mouse gestation. Roa and colleagues (2013) found that dark rearing from late gestation and an *Opn4* mutation produce similar results in terms of vascular development, delaying hyaloid vascular regression, and causing retinal vascular overgrowth. This validates evidence that melanopsin regulates retinal vascular development via a light-dependent pathway. Results of this study point in the direction of manipulating the OPN4 pathway as a potential treatment for ROP.

Human melanopsin has been shown to be maximally responsive to blue light (wavelength of 479 nm) through G-protein signaling cascades (Bailes et al., 2013). If melanopsin is sensitive to blue light and can regulate vascular development, then it seems probable that exposing premature mice to 479-nm light could potentially counter the aberrant neovascularization in ROP.

1.8 Neuropsin and Light

Neuropsin is a photosensitive protein that is encoded by the *Opn5* gene. Little is known about OPN5 other than it responds to violet light (wavelength of 380 nm) and that it mediates retinal circadian photoentrainment (Ota et al., 2018; Buhr et al., 2015). One study presented data suggesting that *Opn5* is critical in the development of the mouse eye by controlling the timing of hyaloid vascular regression (Nguyen et al., 2019). They found that the release of dopamine into the vitreous is influenced by an *Opn5* light pathway, with increased vitreous dopamine and precocious hyaloid vessel regression in *Opn5* knockout mice. Dopamine acts directly on vascular endothelial cell dopamine D2 receptors to promote hyaloid regression.

Vitreous dopamine regulation via a light-dependent pathway occurs simultaneously with increasing levels of dopamine in the postnatal eye. This suggests that dopamine promotes the regression of hyaloid vessels and that the effect of the 380-nm light counters regression of hyaloid vessels. The study noted that OPN4 works similarly in conjunction with VEGF-A to regulate the timing of retinal vascular development. As noted by Rao et al. (2013), OPN4 activation is at prime during late gestation. This indicates that 380-nm light via OPN5 and 480-nm light via OPN4 serve as cues for the development of retinal vasculature. With previous

evidence suggesting that increased ADL reduces the risk of severe ROP, it is possible that insufficient light to the OPN5 pathway could play a role because it results in elevated levels of vitreous dopamine and precocious hyaloid regression. Consistent with this hypothesis, administration of dopamine to treat hypotension associated with prematurity increases the severity of ROP (Hussein et al., 2014).

2. Objective and Hypothesis

It is hypothesized that the manipulation of OPN4 and OPN5 can be used to reduce neovascularization of a mouse model of retinopathy of prematurity. In addition, we hypothesize that altering the wavelength of lights that postnatal mice are exposed to will counter the neovascularization that occurs when newborn mice are exposed to hyperoxia and then returned to normal oxygen conditions. This project is the first set of experiments in the entire investigation of light therapy and OIR. More specifically, it is the first project in the Iuvone lab to attempt to induce retinopathy in neonatal mice. Therefore, the first objective of this investigation was to model OIR in wild type (WT) and genetically modified mice using the method developed by Smith et al. (1994). Although light therapy to target melanopsin and neuropsin encoding genes was not investigated in this project, OIR was modelled in C57BL/6J WT mice. Additionally, OIR was modelled in melanopsin (*Opn4*) and neuropsin (*Opn5*) mice, with preliminary data for *Opn4* heterozygotes (*Opn4* $^{-/+}$) and wild type (*Opn4* $^{+/+}$) mice. The second objective is to use Imaris imaging software to develop a semi-automated way to accurately quantify vasculature. The results from this method will be compared against those provided using cell fluorescence detection on ImageJ, a commonly used technique for analyzing

vasculature. We hypothesize that all OIR mouse models, regardless of genotype, will demonstrate quantifiable differences in the spatial organization of vasculature at P17 due to vaso-obliteration and neovascularization.

3. Methods

3.1 Study Approval and Subjects

This study complies with all relevant ethical regulations regarding animal research. All animals were maintained in a temperature-controlled environment on a 12 h light-dark cycle (light onset at 7:00 A.M.) with food and water provided *ad libitum*. All procedures were approved by the Emory University Institutional Animal Care and Use Committee (IACUC) and conformed to the ARVO Statement for the Use of Animals in Ophthalmic and Vision Research. Day of birth is defined as P1.

C57BL/6J pregnant mice were ordered from Jackson Laboratories and offspring from these mice were used as controls. The genetically modified mice for this project were bred to have the *Opn4* and *Opn5* allele knocked out, with the possibility of having heterozygotes (HT) and WT mice in each litter. *Opn4*$^{tm1.1Yau}$/ J mouse strain (Jackson Laboratory, Jax stock #021153) were developed using 129 embryonic cells, bred to C57BL/6J, and maintained on a mixed background (Hattar et al., 2002). *Opn5*$^{-/-}$ line was generated by using an embryonic stem cell clone from the International Knockout Mouse Consortium (Cincinnati Children's Hospital Medical Center). Conventional methods were used to generate an *Opn5*$^{flox/flox}$ mouse line from these ES cells, which was then crossed to *ROSA-FLP* mice (stock no. 003946; The Jackson Laboratory) and, subsequently, *EIIa-Cre* mice (stock no. 003314; The Jackson Laboratory; with Cre expression in

germ line) to give the *Opn5*$^{-/-}$ line (Buhr et al., 2015). Knockout (KO) mice were bred in the laboratory according to breeding guidelines set by the Division of Animal Resources at Emory University. Ear clippings for these mice were collected for genotyping. The genotyping protocol for the *Opn4* allele is outlined on Jackson Laboratory website. The primer sequences for this line are 5'-AGG CTG GAT GGA TGA GAG C-'3, 5'-GTT GTG AAG CTG GGA TCC TG-'3, and 5'-GGT CTT CCA GGT TGG ATG T -'3. The KO band appears at 490 bp and the WT band appears at 187 bp, while heterozygotes present both bands. The primer for the *Opn5* allele are F1: 5′-CAC AGT ATG TGT GAC AAC CT-3′, R1: 5′-GTG GAC AGA TTA ACT GAA GC-3′, F2: 5′-ACT ATC CCG ACC GCC TTA CT-3′, and R2: 5′-GAA CTG ATG GCG AGC TCA GA-3′. Although both genetically modified lines of mice were bred and OIR induced, only preliminary analysis on data from the *Opn4* line has been conducted at this point. All mice were kept in room air at 21% oxygen before neonates were born. Dams were kept with pups until the day of sacrifice at either P12 or P17.

3.2 OIR Protocol

Oxygen-induced retinopathy, the experimental model for ROP, was applied to newly born C57BL/6J WT mice and the line of *Opn4* and *Opn5* mice according to the protocol developed by Smith et al. (1994). In the experimental group, mice were kept in room air (21% oxygen) from P1 until P7. At P7, neonates and their dams were transferred to a BioSpherix Proox Model 110 Hyperoxia Chamber (BioSpherix, Ltd., cat. no. A-30274) where concentration of oxygen was set at 75% oxygen. After 5 days in the chamber, the mice were returned to room air from P12 to P17. Mice were euthanized with CO_2 at either P12 or P17 in order to compare retinas at different stages of retinopathy. The superior of eyes at the limbus was marked with a cautery

tool and eyes were enucleated. Immediately after removal, eyes were frozen in 10 mL of a 97% methanol 3% acetic acid solution and maintained in -80°C freezer for 2-5 days until flatmounts were prepared.

3.3 Whole Retina Flatmounting

Gap slides were prepared by first using a scribe to cut a #1.5 24x50mm coverslip in half. Each half of the coverslip was glued 1.5 cm away from each other on a slide. Gap slides were dried overnight to ensure a stable flatmounting surface. Tubes with enucleated eyes were brought to room temperature and washed 3x with PBS. Under a microscope, a small radial cut is made perpendicular to the limbus where superior is marked. An eye cup is made by cutting along the limbus and isolating the retinal tissue from the iris, cornea, and lens. The eye cup is placed in a 2 ml tube with 300 µl of PBST and 1.5 µl of Lycopersicon esculentum (tomato) lectin-LEA, DyLight 488 staining (Invitrogen by Thermo Fisher Scientific; Eugene, Oregon, USA) and allowed to incubate overnight in a dark room. The following day, the eye cup is washed 3x in PBS with 5 minutes between each wash to remove excess staining. Under red light, radial cuts were made from the periphery of the eye cup towards the head of the optic nerve to split the retina into 4 quadrants. Once the retina is flattened on the gap slide in the space between the halved cover slip, 3-4 drops of Vectashield Vibrance Antifade Mounting Medium with DAPI (Vector Laboratories; Burlingame, USA, CA) is added to the retina. A cover slip is placed over the top. The perimeter of the cover slip is secured onto the gap slide using nail polish. The gap slides are allowed to dry overnight before being imaged.

3.4 Microscopy

Wholemount retina images were acquired using the Nikon A1 camera on the Nikon Ti2 with A1RHD25 confocal microscope (Nikon, New York, NY, USA). A 20x objective lens was used with four lasers (405 nm, 488 nm, 561 nm, 640 nm) allowing for acquisition of confocal data for different excitation wavelengths. The values for Z-stack were set as follows: Z-stack bottom at -30, Z-stack top at 30, and Z-stack steps at 2.5.

3.5 Quantification of Vasculature

A novel method of analyzing retinal vasculature with Imaris was developed and is outlined below. This method is compared against an established method of quantifying cell fluorescence using ImageJ.

Loading the image onto the Imaris software, the 3D/4D visualization allows for vasculature tracing on Imaris Surpass. A new filament was created using the Filament Tracer in Autopath mode. On each of the 4 quadrants on the retinal flat mount image, two 636µm x 636µm regions of interest (ROI) were selected. One was placed 800µm from the optic nerve head to measure the central vasculature and the other was placed 800µm from the first ROI to measure peripheral vasculature (Fig. 1). Imaris displays three dendrite source channels and the green channel (channel 2) was selected to detect the green fluorescence produced by the isolectin staining. Next, the image was visualized in “Slice Mode” to measure the maximum diameter of a vessel and these values were then inputted as “Start Point” and “End Point” in filament tracer mode. Since the Imaris Filament Tracer is designed for neuron tracing, the automatic threshold for detecting seed and starting points will make an overestimate. Automatic detection was

overridden by sliding both threshold bars to the right until no seed points remain. The starting and seed points were manually entered, using as few points as possible to prevent the software from overestimating. “Remove Disconnected Segments” function was activated to disconnect separate vessels that were mistaken as the same vessel. In order to correct any mistakes made from entering seed points manually, “Background Subtraction” was applied. This applies a Gaussian Filter to define the background at each background and subtract any variable background. The threshold for background subtraction and dendrite diameter were set at the maximum limit because this level best represented the actual structure of the vessel. Imaris then produced a traced vessel that matches the original fluorescence. The statistics section displays the vascular area, vascular volume, and branch points.

A previously developed protocol was followed to measure the cell fluorescence of the whole retina using ImageJ (Hammond, 2014). The Polygonal tool was used to trace the perimeter of the retina. With the “area integrated intensity” and “mean grey value” selected, the Analyze function is used to calculate a stack of values. Next, three regions on the image with no cell fluorescence were selected and analyzed. Using the following formula, corrected total cell fluorescence (CTCF) was found:

$$CTCF = Integrated\ Density - (Area\ of\ Selected\ Cell * Mean\ Fluorescence\ of\ Background)$$

3.6 Statistical Analysis

All data was analyzed using PRISM software (Version 8.2; GraphPad Software, La Jolla, CA, USA). The data generated from Imaris was analyzed using a two-way analysis of variance (ANOVA) and

Tukey's multiple-comparison posttest. ImageJ data was analyzed using an unpaired two-tailed t-test. Differences between groups were considered to be significant at a *P* value of <0.05.

4. Results

4.1 Visual Comparison Between C57BL/6J WT Room Air (RA) vs. OIR Images at P17

With the whole retina flat mount protocol, the 3D structure of the vascular network is converted to a 2D image with retinal layers stacked and compressed on each other. The staining allows for visualization of endothelial cells in the superficial and deep layers of the retina. Images of the RA C57BL/6J retinas at P17 represent the expected architecture of a healthy retina. There is observable radial branching in the vessels along with minimal gaping in the retinal tissue (Fig. 1A-B). In comparison, OIR C57BL/6J retinas at P17 consistently presented as less fluorescent blood vessels with obvious pockets of space with no subretinal or retinal vasculature (Fig. 1A-B). With a consistent staining protocol used on all retinas, it is visually obvious that the mouse retina is susceptible to oxygen perturbations. However, the OIR retinas at P17 did not present with the observable and predicted central zone of vaso-obliteration nor with signs of neovascular tufts in the periphery. Further analysis with Imaris and ImageJ will offer a morphometric comparison of the vascular network in RA *vs*. OIR mice.

RA C57BL/6J WT **OIR C57BL/6J WT**

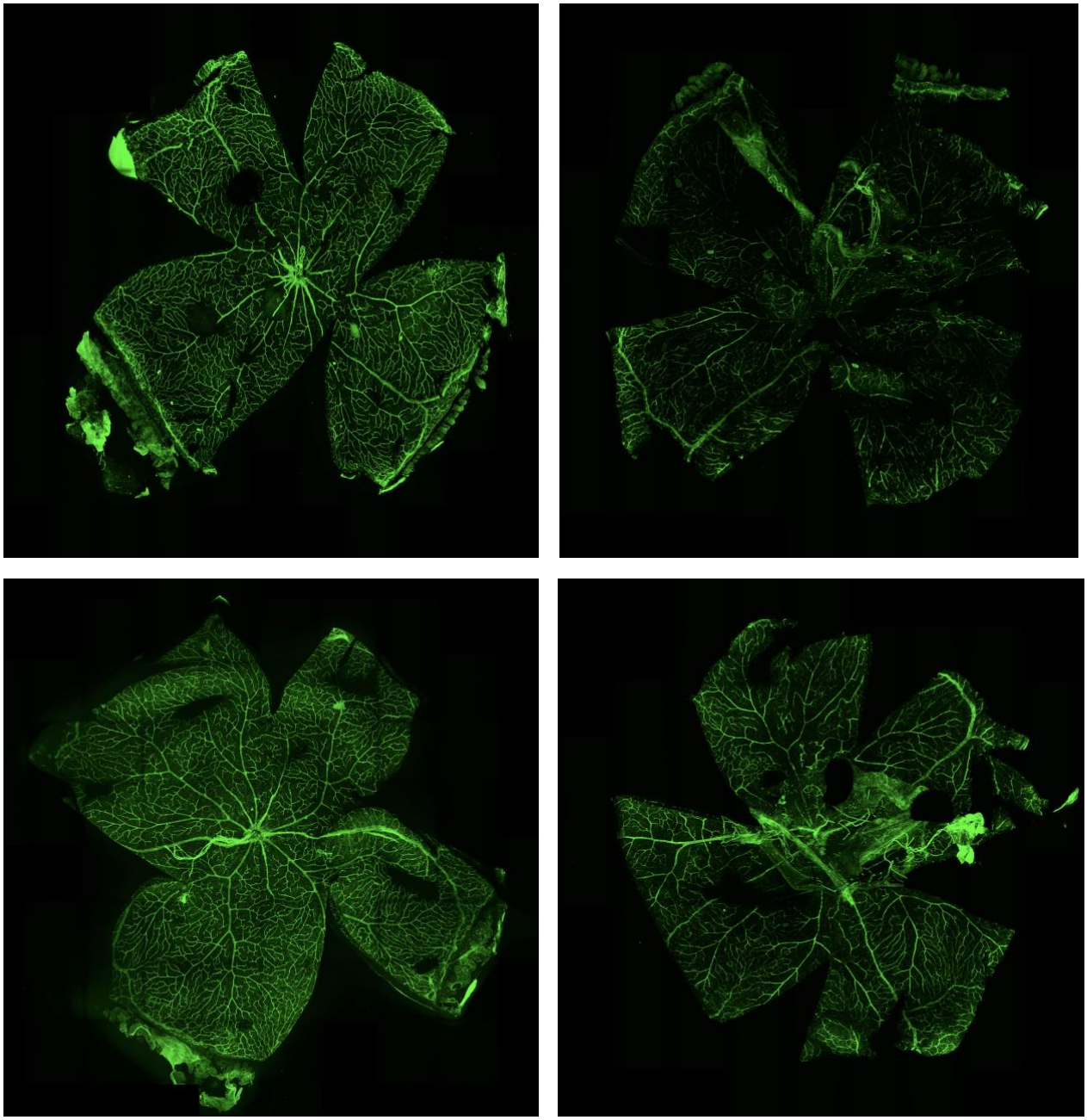

Figure 1A: RA *vs.* OIR C57BL/6J WT retina flatmounts: Images of Lycopersicon esculentum (tomato) lectin-LEA stained RA and OIR retinal flatmounts at P17.

RA C57BL/6J WT **OIR C57BL/6J WT**

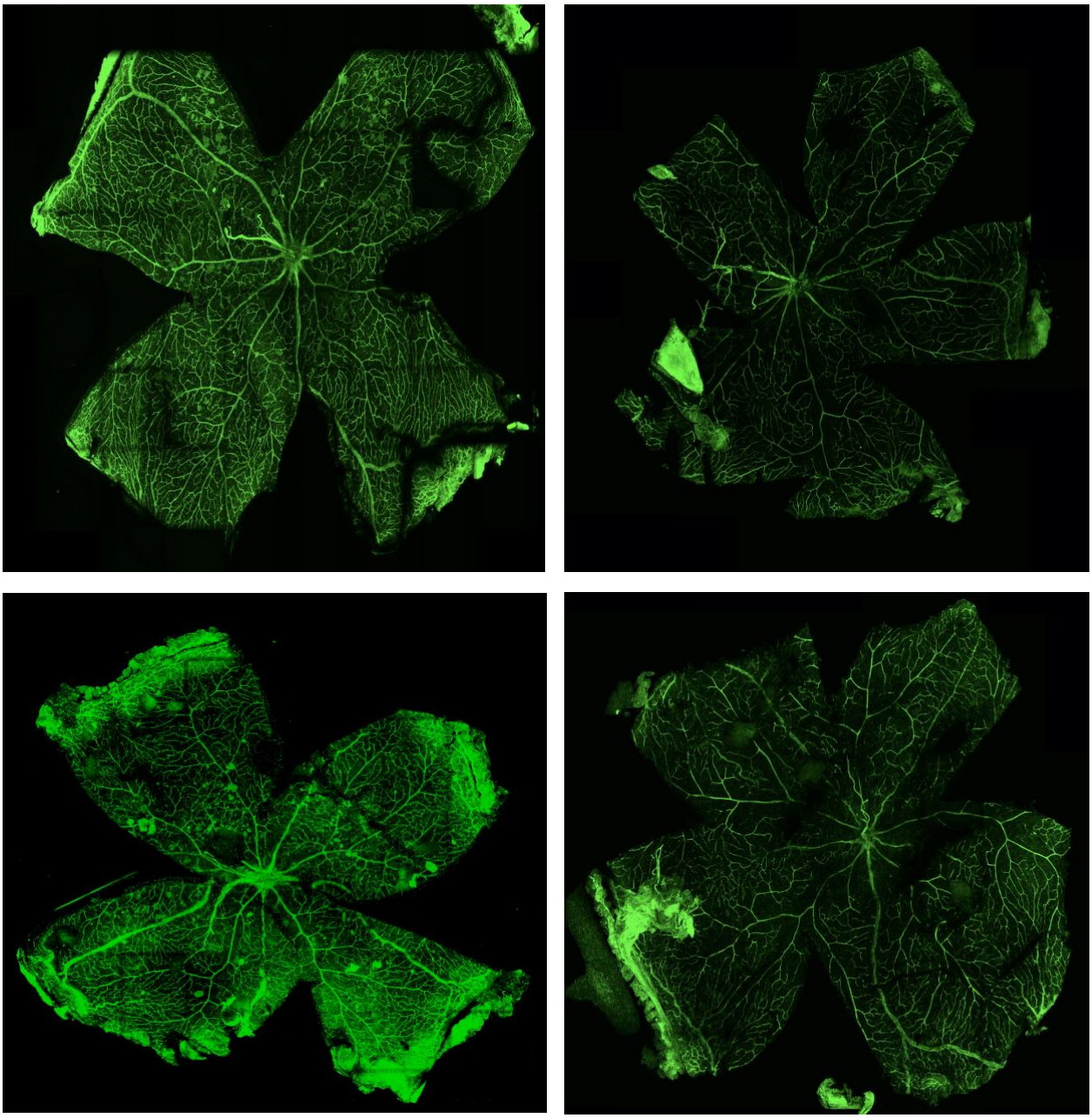

Figure 1B: RA *vs.* OIR C57BL/6J WT retina flatmounts: Images of Lycopersicon esculentum (tomato) lectin-LEA stained RA and OIR retinal flatmounts at P17.

4.2 Morphometric Quantification of C57BL/6J WT Retinas with Imaris

Vascular development in C57BL/6J WT was more robust in P17 RA mice than P17 OIR mice. In total, eighteen retinas (RA: n=9, OIR: n=9) were analyzed with Imaris software for total vascular area, vascular volume, and branch point (Fig. 2 A-F). Imaris enables users to view the vacualture from a 3D/4D perspective as seen in Figure 2. The data from central and peripheral regions of interest were separated to account for the spatial specificity of vaso-obliteration and neovascularization. Imaris analysis revealed that RA vasculature occupied a significantly greater area of space in the central ($p \leq 0.05$) and peripheral retina ($p \leq 0.001$) than OIR vasculature (Fig. 3). The vessels in RA mice were significantly more volumetric in the central ($p \leq 0.05$) and peripheral retina ($p \leq 0.001$) than OIR mice (Fig. 4). Following the same trend, there was significantly more branching in the central and peripheral retina ($p \leq 0.0001$) in RA vasculature than OIR (Fig. 5). There was no significant difference in area, volume, or branch points between central and peripheral zones in the RA models. Similarly, there was no significant difference in area, volume, or branch points between central and peripheral zones in the OIR models. With no significant difference between central and peripheral zones in OIR mice, there is no evidence of the tell-tale signs of OIR (vaso-obliteration and neovascularization) in WT C57BL/6J at P17. However, the significant difference in retinal properties between RA and OIR mice indicate that some degree of retinopathy is being induced at P17. This prompts a closer look at the timing of vascular regression and prominence of vasa-obliteration and neovascularization at P17 in C57BL/6J mice.

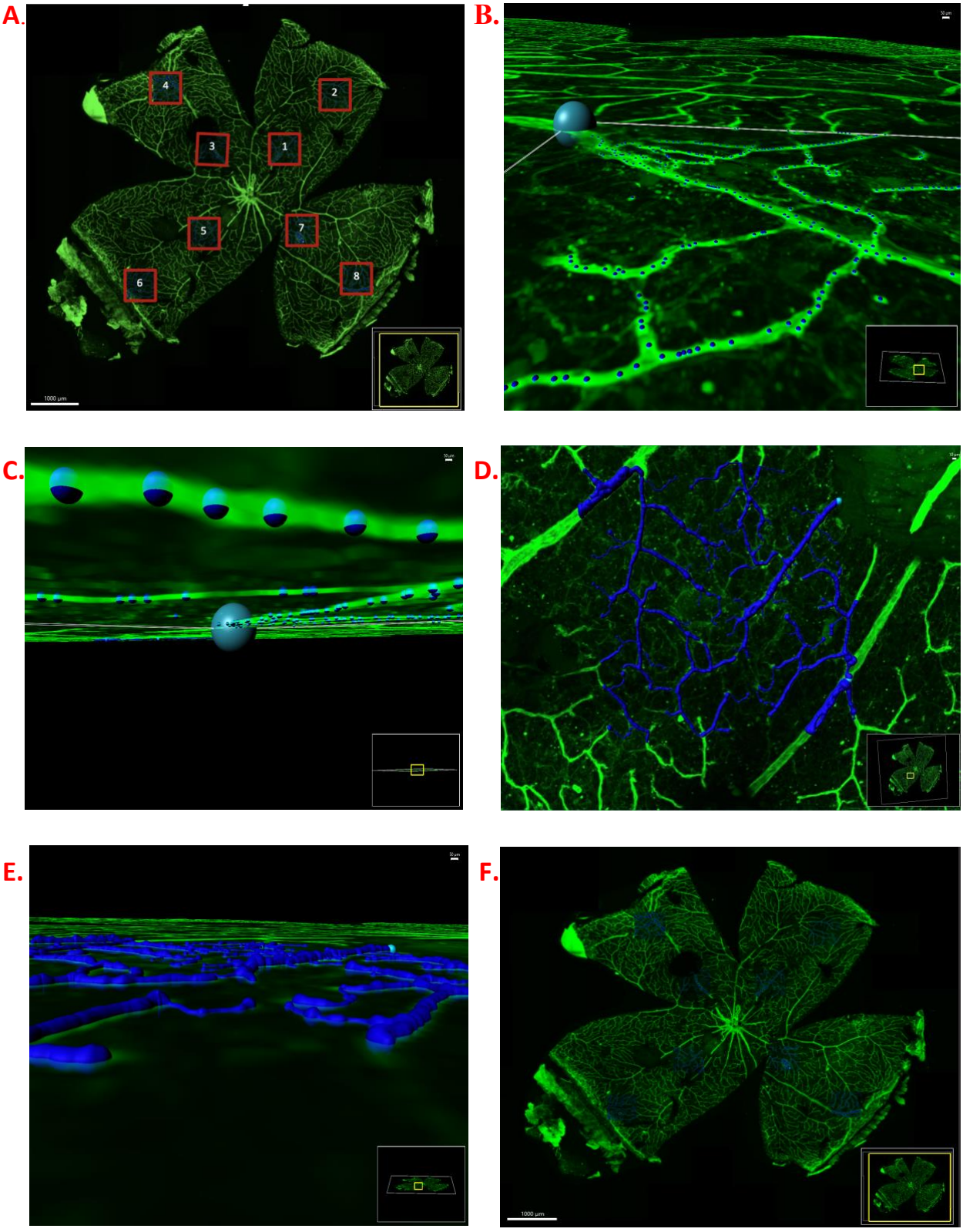

Figure 2. Analysis of flatmounts using Imaris software. (A) Flatmount illustrating the eight regions of interests analyzed in relation to the center and periphery. (B) Region of interest upon selection of starting point and seed points. (C) 3D visualization of the starting point and seed points. (D) Vasculature of region of interest traced in blue. (E) 3D visualization of vasculature traced in blue. (F) Final flatmount after Imaris analysis of eight regions of interests.

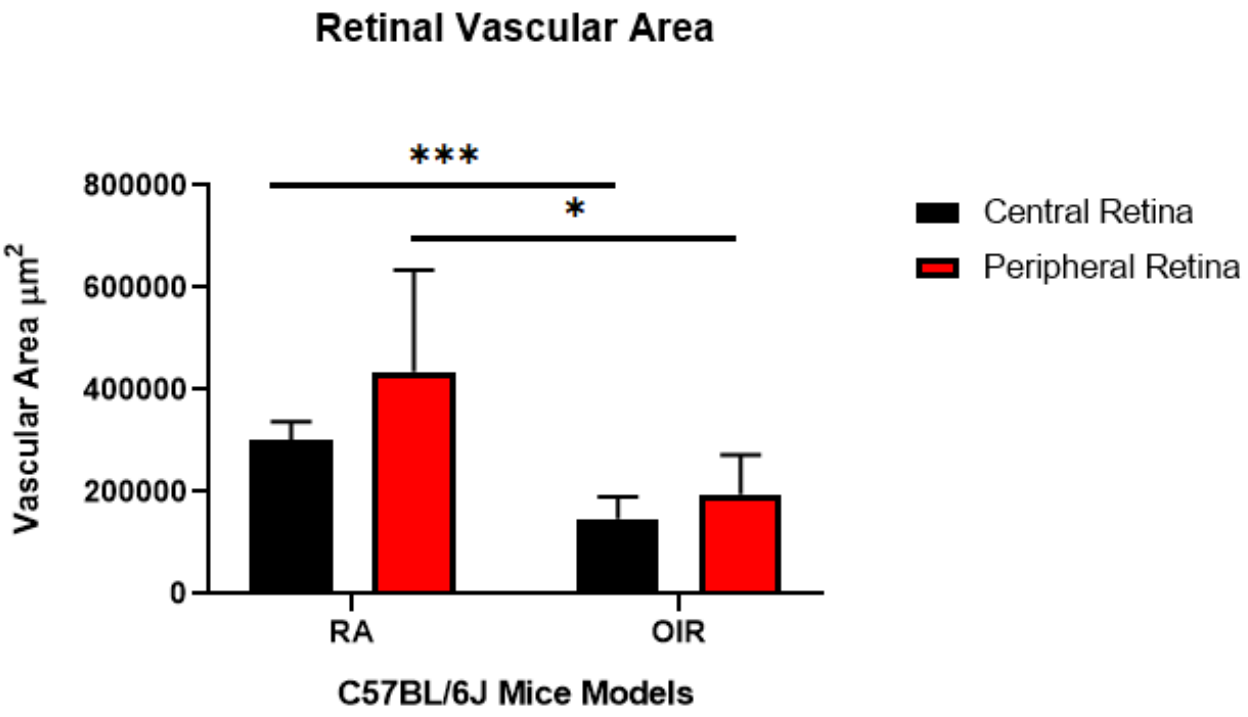

Figure 3. Vascular area in central and peripheral retina in RA *vs.* OIR Mice. Mean area occupied by vasculature in 636µm x 636µm regions of interest in the central and peripheral retina. Data retrieved from Imaris analysis. Significantly greater area of vasculature in RA than OIR mice in both the central and peripheral retina. *$p \leq 0.05$ in RA vs. OIR central retina, ***$p \leq 0.001$ in RA vs OIR peripheral retina; n=9 per group (RA/OIR).

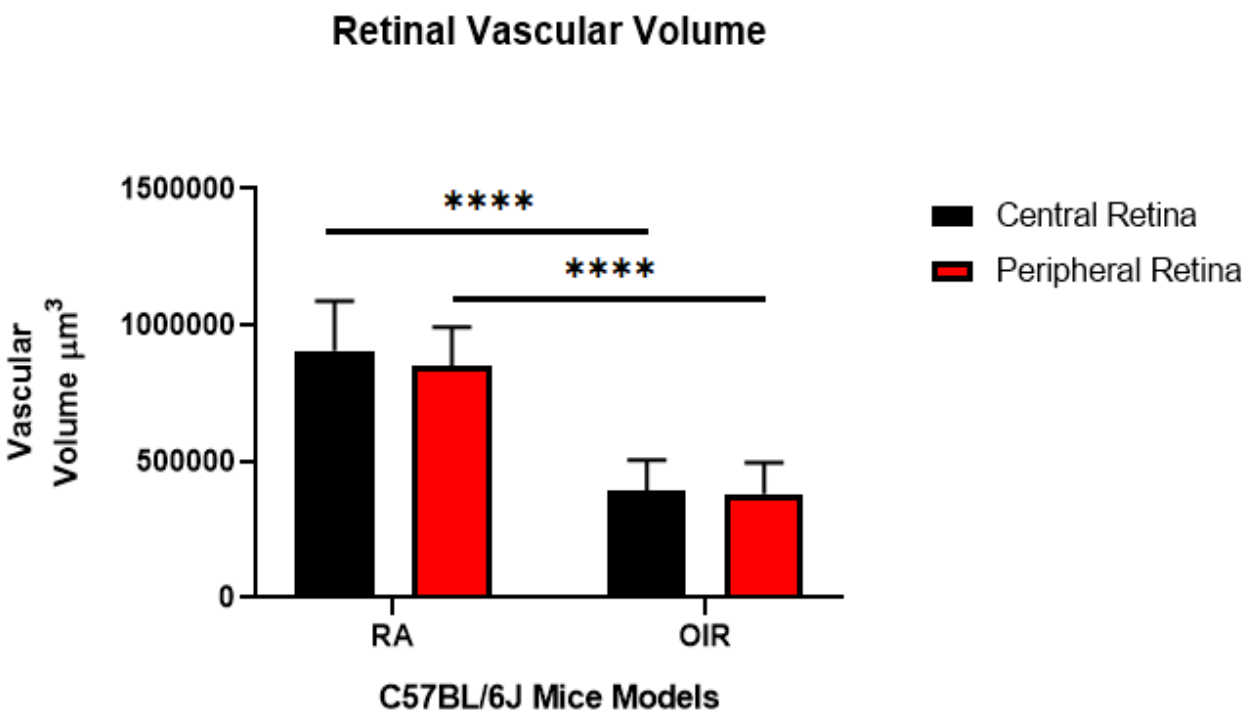

Figure 4. Vascular volume in central and peripheral retina in RA *vs.* OIR Mice. Mean volume occupied by vasculature in 636µm x 636µm regions of interest in the central and peripheral retina. Data retrieved from Imaris analysis. Significantly greater volume of vasculature in RA than OIR mice in both the central and peripheral retina. ****p ≤ 0.0001 in RA vs. OIR central and peripheral retina; n=9 per group (RA/OIR).

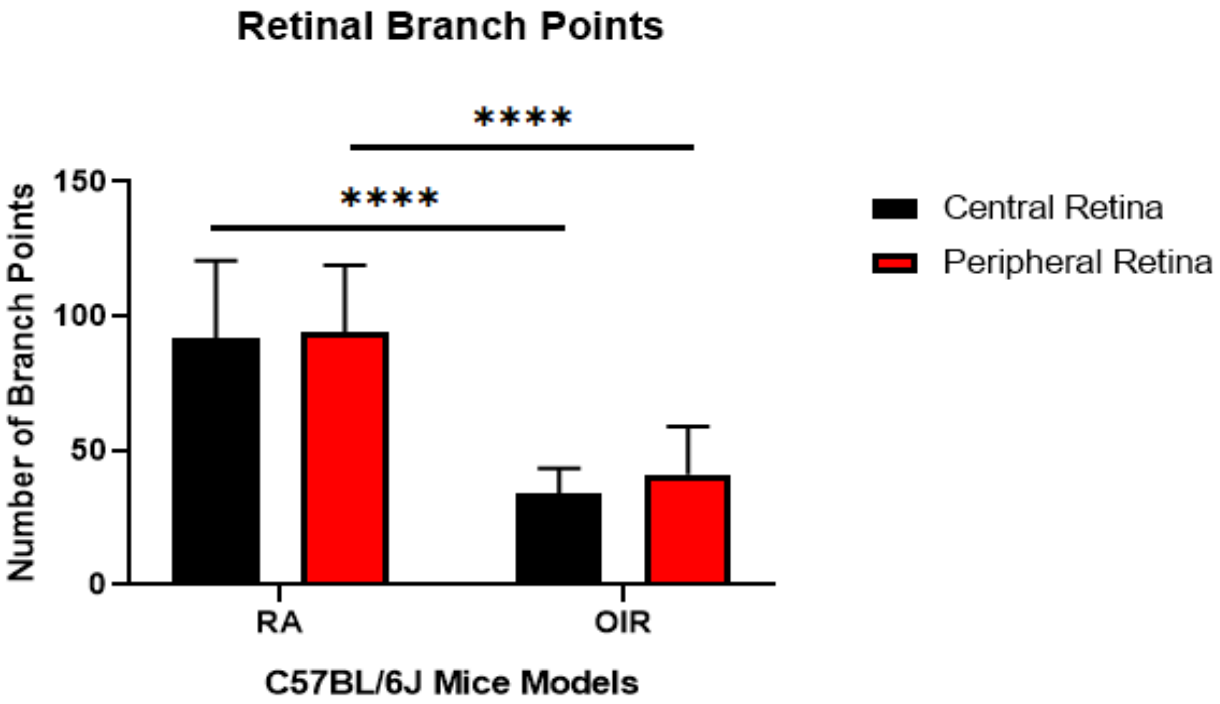

Figure 5. Number of branch points in central and peripheral retina in RA *vs.* OIR Mice. Mean count of branch points 636µm x 636µm regions of interest in the central and peripheral retina. Data retrieved from Imaris analysis. Significantly greater number of branch points in RA than OIR mice in both the central and peripheral retina. ****$p \leq 0.0001$ in RA vs. OIR central and peripheral retina; n=9 per group (RA/OIR).

4.3 *Quantification of C57BL/6J WT Retinas with ImageJ*

The images analyzed with Imaris were also quantified for CTCF with ImageJ software to compare the general trend of results to a more established method of analysis. CTCF quantification does not measure a morphological feature, rather it quantifies the level of fluorescence of the image. Therefore, analysis with ImageJ not only validates the Imaris technique, but considers a different feature of the retinal flatmount entirely. Whole retinas were analyzed for CTCF rather than regions of interest to evaluate how the compounded effects of vaso-obliteration and neovascularization influence total retinal vasculature. The CTCF was calculated after obtaining the integrated density, area, and mean fluorescence of background readings. ImageJ analysis indicated significantly greater CTCF in RA C57BL/6J WT mice than OIR models (Fig. 6). This result affirms that induced retinopathy is altering retinal development in OIR C57BL/6J WT mouse models.

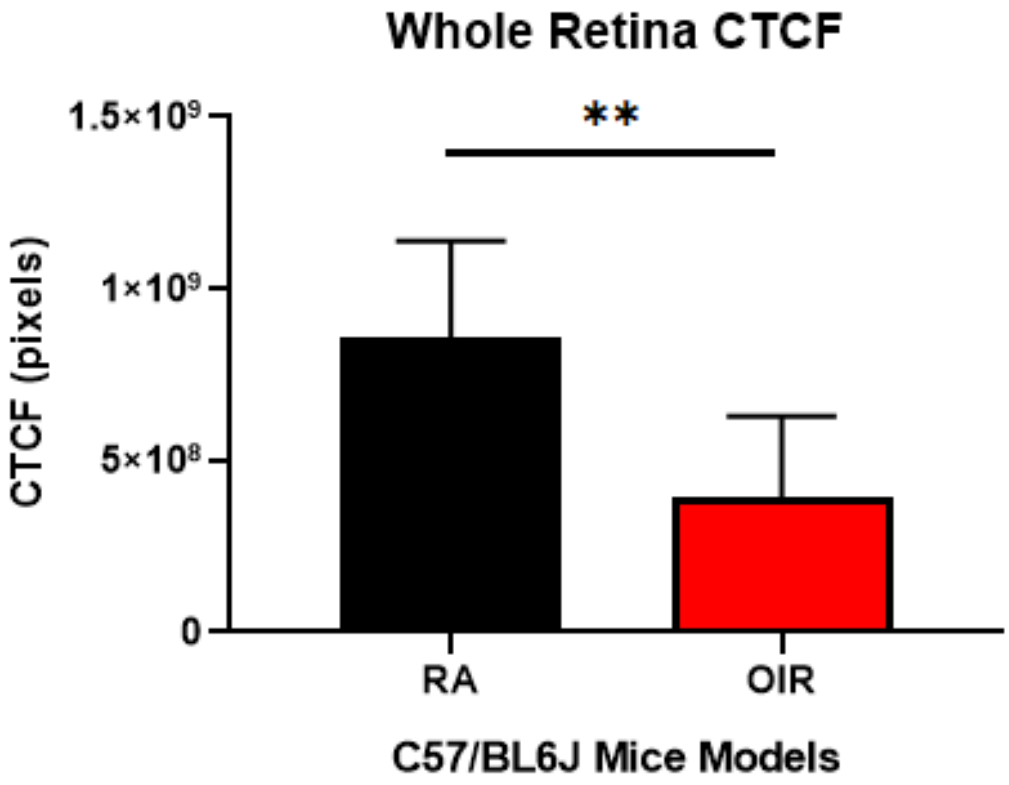

Figure 6. Whole Retina CTCF in RA vs. OIR Mice. Data retrieved from ImageJ analysis. Significantly greater CTCF in RA than OIR mice.**p ≤ 0.01 in RA *vs.* OIR; n=9 per group (RA/OIR).

4.4 *Visual Comparison Between Opn4 wild type(WT; Opn4$^{+/+}$) and heterozygous (HT; Opn4$^{-/+}$) mice: RA vs. OIR Images at P12*

The results from genotyping the *Opn4* line indicated that all of the mice were either WT (*Opn4*$^{+/+}$) with a C57BL/6J background or HT (*Opn4*$^{-/+}$). Analysis of the WT C57BL/6J RA and OIR mice suggested that vaso-obliteration had partially resolved by P17; therefore, half the neonates from the *Opn4* line were sacrificed at P12 and the other half at P17. At this point, only 4 retinas at P12 from the *Opn4* line have been imaged: RA *Opn4*$^{+/+}$, OIR *Opn4*$^{+/+}$, RA *Opn4*$^{-/+}$, OIR *Opn4*$^{-/+}$(Fig. 7). The low *n* value makes it difficult to analyze these images for significance, but the visual features of the retinas are highly indicative of OIR. In both the OIR *Opn4*$^{+/+}$ and OIR *Opn4*$^{-/+}$ retinas, a zone of vaso-obliteration is prominent in the central retina. In the RA *Opn4*$^{+/+}$ and RA *Opn4*$^{-/+}$, the superficial vascular plexuses developed uniformly from the center to the periphery. The primary vasculature that extends from the head of the optic nerve can still be seen in the OIR retinas, but the branching network that extends from the primary vessel is absent. The vaso-obliteration created an avascular zone in the OIR models.

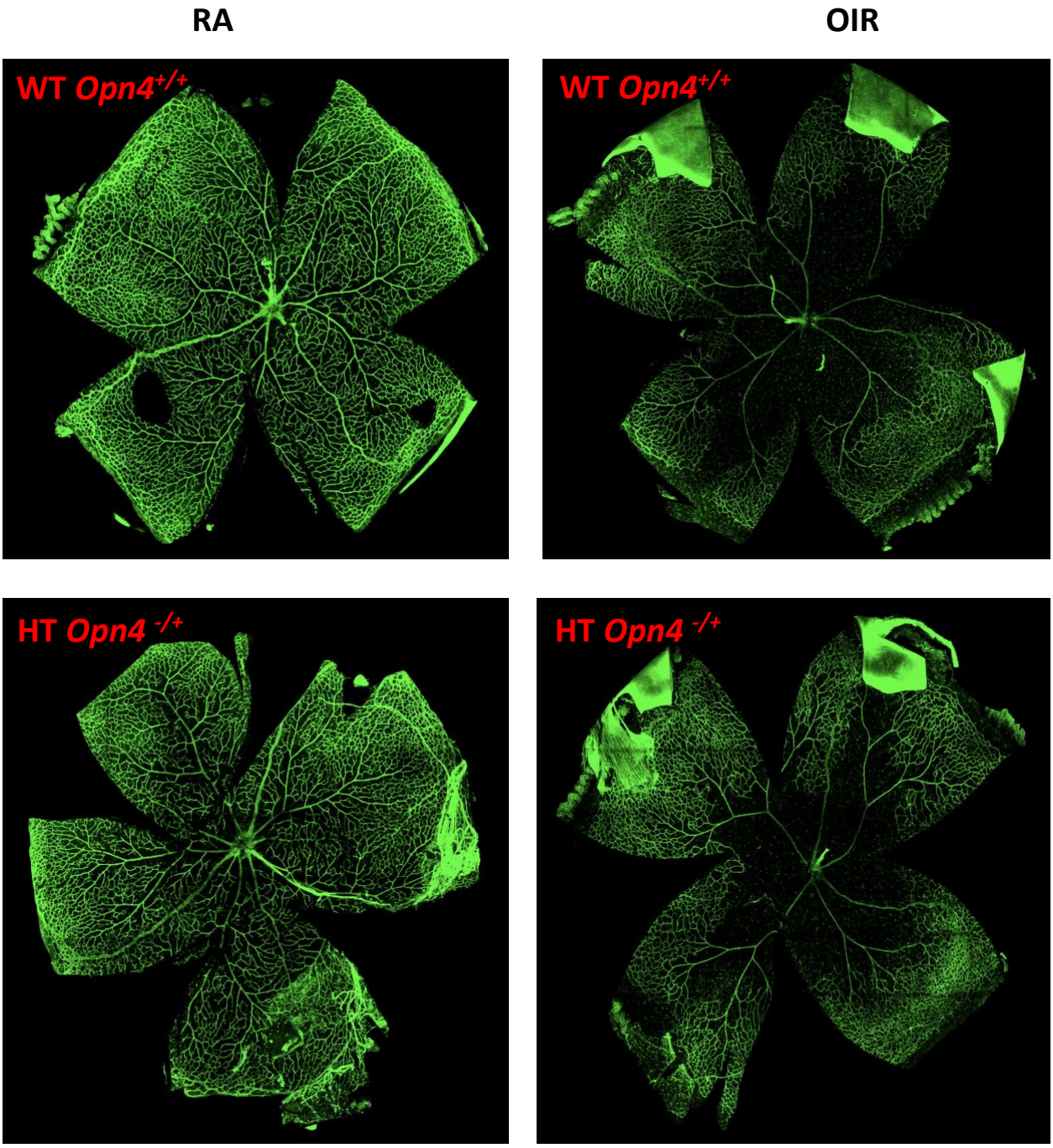

Figure 7. RA and OIR *Opn4* WT/HT retina flatmounts: Images of Lycopersicon esculentum (tomato) lectin-LEA stained RA and OIR retinal flatmounts at P12.

5. Discussion

Large scale studies have concluded that advancements in neonatal care are increasing the survival rate of preterm infants and, consequently, leading to a significant rise in the incidence of ROP (Freitas et al., 2018). Evaluation of therapies that target aberrant vessel growth to restore the architecture of a healthy retina are crucial in mitigating the potentially debilitating consequences of the disease. With vascular development being a highly orchestrated and complex process, animal models are an imperative mode of study before relaying therapies to the clinical stage. The timeline of vascular development in the mouse retina makes it an exploitable model for studying the pathophysiological features of ROP. The mouse retina offers an avenue for investigating treatment options for ROP that has been utilized by researchers for the past 25 years (Smith et al., 1994). It is equally important that techniques for quantifying changes in the retina are simultaneously developed. In this study, OIR was induced in WT C57BL/6J mice, *Opn4*$^{+/+}$, and *Opn4*$^{-/+}$. Additionally, a novel technique for analyzing the 3D structure of the vasculature was created to accurately report on how these retinas respond to oxygen perturbations. This study is a launching point for a series of projects that will explore light-activation of melanopsin and neuropsin as a treatment for OIR in mice.

Our results suggest that the wild type mice (C57BL/6J) in the control (RA) and experimental (OIR) groups had significant differences in retinal vascular development. The novel technique developed via Imaris indicates that mice subjected to hyperoxic conditions had retinal vessels that occupied a smaller area, were less volumetric, and exhibited fewer branch points. ImageJ both confirmed this method of analysis and evaluated a different feature of the retina with the

conclusion that experimental retinas exhibited more cell fluorescence in relation to the background. Significant results from two modes of analysis are evidence that the OIR protocol is inducing some level of retinopathy in these mice. Although a comparison between regions of OIR retinas and those respective regions in control mice revealed significance, this is not indicative of vaso-obliteration or neovascularization. Regardless of the fact that there was overall less vasculature in OIR models, the lack of variation between the center and periphery of the OIR retinas implies that neither neovascularization or vaso-obliteration are apparent at P17.

According to current literature, the established timeline of the OIR mechanism in a mouse model is as follows: initial vessel loss (P7-P12), neovessel formation (P12-P17), and vascular regression (P17-P25). Therefore, vaso-obliteration in the central retina is at a maximum at P12 while neovascularization in the peripheral retina is at a maximum at P17. A study by Li et al. (2012) found that the avascular zone reduced significantly from P12 to P17. The study cited that the avascular zone compromised 47.1% of the total retina at P12, but only 16.4% of the total retina at P17. Similarly, Chikaraishi et al. (2007) noticed that the capillary-free zone diminished by 15% from P12 to P17. Although both of these studies modelled OIR in mice with different genetic backgrounds than C57BL/6J, they present findings of a non-discrete central zone of vaso-obliteration at P17. It is possible that the vasculature regresses faster than expected with the avascular zone partially resolved by P17. On the other hand, it is abnormal to not be able to clearly visualize neovascularization in the periphery at P17. This may be a result of a limitation with Imaris software. The Imaris software traditionally analyzes neuronal bodies with clear somas, dendrites, and axons. Retinopathy induced vasculature creates neovascular tufts, which are multinucleated structures that project into the vitreous. The filament tracer on Imaris may

Imaris may be unable to trace the irregularities of these structures leading to inaccurate quantification. Another potential reason for lack of neovascularization could be that the parts of the periphery were cut off during dissections. Perhaps creating an eye cup that extends to the cornea could offer a more comprehensive visualization of the retinal tissue.

Analysis of the wild type C57BL/6J mice at P17 led us to take a different approach with the *Opn4* line. Rather than sacrificing all of the neonates at P17, we sacrificed a few mice in each litter at P12. This allowed us to have a visual comparison of the spatiotemporal organization of retinal vasculature at P12. Preliminary visual evidence suggests a drastic difference in the central zone of OIR retinas in comparison to the central zone of room air control retinas. The results from the Opn4 line are preliminary and do not suggest significance; however, they offer initial insight into the timing of retinal angiogenesis in OIR mice. More *Opn4* mice are currently being tested.

5.1 Limitations

Multi-dimensional analysis is especially important in studying OIR, where endothelial cells occupy new spatial arrangements in the form of neovascular tufts. Although the protocol for Imaris analysis lets us observe the retinal structure from a 3D perspective, the configurations of the software only allowed us to create box-shaped regions of interest. This may have hindered the Imaris software from detecting neovascularization. If the software could create rectangular regions of interest, the entire width of each petal could have been analyzed. Neovessel formation is spatially dominant across the peripheral breadth of the retina, so a larger area of interest may offer a more comprehensive analysis of neovascularization.

The technical difficulty of producing retinal flamtounts with clear visualization of the vasculature makes it essential to have high *n* values. Although this study had an adequate sample size for wild type mice, imaging flatmounts was paused for over 2 months with the laboratory's Nikon A1 camera in repair. As a result, one of the greatest limitations in this study was imaging and analyzing the flatmounts in the time frame given. Also, when delineating a phenotype, high *n* values are essential to overcome biological variability. As a result, current literature recommends using knockout mice from three different litters (Connor et al., 2009). This was the intent with the *Opn4* and *Opn5* line, but subsequent imaging of dissected retinas was halted due to equipment malfunction. Thus, the data from the *Opn4* line mice is limited by the low *n* value.

5.2 Future Directions

As mentioned previously, the overarching goal of this study is to manipulate novel opsins via light therapy in wild type and genetically modified mice to counter neovascularization and neuronal dysfunction in ROP. Thoroughly investigating the mechanism and timeline of OIR in these mice and perfecting a method of quantification are essential steps before launching the investigation on treatment. Future OIR experiments should focus on inducing C57BL/6J, *Opn4,* and *Opn5* mice and extracting retinas at P12, P14/P15, P17, and P25. Although there is evidence that vaso-obliteration decreases at a significant rate from P12 to P17 (Li et al., 2012), OIR C56BL/6J mice should continue to be studied to understand why there was little evidence of neovessel formation in the periphery of the retina at P17. Sacrificing the mice at P14 or P15 could be used to compare neovascular tuft formation in the periphery at P17, when

neovascularization is at a maximum. Sacrificing these mice at P12, similarly to the *Opn4* mice, can help confirm that vaso-obliteration has partially resolved by P17 and if vascular regression is occurring earlier than expected. The mouse model of OIR predicts that neovascular growth will regress by P25, so analysis of retinas at this point could provide a benchmark to compare vasculature post treatment. All in all, a collection of retinas from these timepoints will allow us to visualize how OIR manifests based on different stages of development and the genetic background of the mice.

In terms of quantification, the data produced from ImageJ analysis was limited because there was no segmentation of the retina. In a study by Arias et al. (2019), researchers measured intravascular areas in three different concentric circles that were defined based on their distance from the optic nerve. Using a method similar to this would give a more precise quantification of the level of neovascularization and vaso-obliteration. Eventually, a fully automated method of analysis should be adapted to allow for objective quantification. Xiao et al. (2017) developed a software tool that now exists as an open access package for percentage quantification of vaso-obliteration and neovascularization. Although this mode of analysis does not allow for 3D quantification, it will allow us to monitor ocular angiogenesis in a time-efficient manner. A fully automated software will relieve us of the time spent on repetitive quantification that can be better invested on experimental planning.

Once we have a more established understanding of how OIR manifests in C57BL/6J, *Opn4*$^{-/-}$, and *Opn5*$^{-/-}$ mice, experiments should focus on activating novel opsins as a treatment for OIR. With hyaloid vessel regression closely linked to vascular development, triggering a light-dependent

pathway could counter the aberrant growth of vasculature in the retina. To investigate this as a treatment for OIR, mice should be exposed to blue or violet light during and post exposure to hyperoxia (P7-P17). Future experiments would have to determine the hourly length of exposure per day and the distance each mice need to be placed from the light source. The arrangement determined for the mouse models should mimic the effect of exposing preterm infants to blue and violet light immediately after birth.

From a clinical perspective, it is important to note how light therapy *in vivo* could introduce treatment options for improving the prognosis for patients with ROP. In theory, low levels of exposure to different wavelengths of light is non-invasive and inexpensive (Natoli et al., 2013). The current treatments available to human infants with ROP include cryopreservation and laser treatment. These are invasive surgical procedures that destroy the peripheral areas of the retina with aberrant and leaky vasculature (Roohipoor et al., 2009). A major risk of these treatments is inadvertently destroying peripheral vision, hence, why this is only an option for advanced stage candidates. Although 90% of mild cases resolve without treatment, these children are at a higher risk of developing ocular complications like glaucoma, myopia, strabismus, and amblyopia later in life (Rivera et al., 2018). The continued investigation into light-activation of melanopsin and neurospin can potentially yield novel and exploitable insights into future treatments.

References

Arias, J.E.R., Economopoulou, M., López, D.A.J., Kurzbach, A., Yeung, K.H.A., Englmaier, V., Merdausl, M., Schaarschmidt, M., Ader, M., Morawietz, H., Funk, R.H.W., Jászai, J., n.d., 2019. VEGF-Trap is a potent modulator of vasoregenerative responses and protects dopaminergic amacrine network integrity in degenerative ischemic neovascular retinopathy. Journal of Neurochemistry.

Arnesen, L., Durán, P., Silva, J., Brumana, L., 2016. A multi-country, cross-sectional observational study of retinopathy of prematurity in Latin America and the Caribbean. Rev Panam Salud Publica 39, 322–329.

Askie, L.M., Henderson-Smart, D.J., Ko, H., 2009. Restricted versus liberal oxygen exposure for preventing morbidity and mortality in preterm or low birth weight infants. Cochrane Database Syst Rev CD001077.

Bailes, H.J., Lucas, R.J., 2013. Human melanopsin forms a pigment maximally sensitive to blue light (λmax ≈ 479 nm) supporting activation of Gq/11 and Gi/o signaling cascades. Proc Biol Sci 280.

Beauchamp, M.H., Sennlaub, F., Speranza, G., Gobeil, F., Checchin, D., Kermorvant-Duchemin, E., Abran, D., Hardy, P., Lachapelle, P., Varma, D.R., Chemtob, S., 2004. Redox-dependent effects of nitric oxide on microvascular integrity in oxygen-induced retinopathy. Free Radical Biology and Medicine 37, 1885–1894.

Bodnar, R.J., 2014. Anti-Angiogenic Drugs: Involvement in Cutaneous Side Effects and Wound-Healing Complication. Advances in Wound Care 3, 635.

BOOST II, BOOST II, BOOST II, 2013. Oxygen saturation and outcomes in preterm infants. N Engl J Med.368:2094–2104.

Buhr, E.D., Yue, W.W.S., Ren, X., Jiang, Z., Liao, H.-W.R., Mei, X., Vemaraju, S., Nguyen, M.-T., Reed, R.R., Lang, R.A., Yau, K.-W., Gelder, R.N.V., 2015. Neuropsin (OPN5)-mediated photoentrainment of local circadian oscillators in mammalian retina and cornea. PNAS 112, 13093–13098.

Carlo, W.A., Higgins, R.D., 2010. Optimum oxygen therapy to prevent retinopathy of prematurity. Expert Rev Ophthalmol 5, 583–585.

Chang, M., 2011. Optimal oxygen saturation in premature infants. Korean J Pediatr 54, 359–362.

Chen, M.L., Guo, L., Smith, L.E.H., Dammann, C.E.L., Dammann, O., 2010. High or low oxygen saturation and severe retinopathy of prematurity: a meta-analysis. Pediatrics 125, e1483-1492.

Chikaraishi, Y., Shimazawa, M., Hara, H., 2007. New quantitative analysis, using high-resolution images, of oxygen-induced retinal neovascularization in mice. Experimental Eye Research 84, 529–536.

Connor, K.M., Krah, N.M., Dennison, R.J., Aderman, C.M., Chen, J., Guerin, K.I., Sapieha, P., Stahl, A., Willett, K.L., Smith, L.E.H., 2009. Quantification of oxygen-induced retinopathy in the mouse: a model of vessel loss, vessel regrowth and pathological angiogenesis. Nat Protoc 4, 1565–1573.

Dorrell, M.I., Friedlander, M., 2006. Mechanisms of endothelial cell guidance and vascular patterning in the developing mouse retina. Progress in Retinal and Eye Research 25, 277–295.

Eglen, S.J., Raven, M.A., Tamrazian, E., Reese, B.E., 2003. Dopaminergic amacrine cells in the inner nuclear layer and ganglion cell layer comprise a single functional retinal mosaic. J Comp Neurol 466, 343–355.

Freitas, A.M., Mörschbächer, R., Thorell, M.R., Rhoden, E.L., 2018. Incidence and risk factors for retinopathy of prematurity: a retrospective cohort study. Int J Retina Vitreous 4.

Hammond, L., 2014. Measuring cell fluorescence using ImageJ. The Open Lab Book.

Hattar, S., Liao, H.-W., Takao, M., Berson, D.M., Yau, K.-W., 2002. Melanopsin-Containing Retinal Ganglion Cells: Architecture, Projections, and Intrinsic Photosensitivity. Science 295, 1065–1070.

Hussein, M.A., Coats, D.K., Khan, H., Paysse, E.A., Steinkuller, P.G., Kong, L., O'Brian, S.E., 2014. Evaluating the association of autonomic drug use to the development and severity of retinopathy of prematurity. Journal of American Association for Pediatric Ophthalmology and Strabismus 18, 332–337.

Johnson, J., Wu, V., Donovan, M., Majumdar, S., Rentería, R.C., Porco, T., Gelder, R.N.V., Copenhagen, D.R., 2010. Melanopsin-dependent light avoidance in neonatal mice. PNAS 107, 17374–17378.

Kim, C.B., D'Amore, P.A., Connor, K.M., 2016. Revisiting the mouse model of oxygen-induced retinopathy. Eye Brain 8, 67–79.

Li, J., Wang, J.J., Peng, Q., Chen, C., Humphrey, M.B., Heinecke, J., Zhang, S.X., 2012. Macrophage Metalloelastase (MMP-12) Deficiency Mitigates Retinal Inflammation and Pathological Angiogenesis in Ischemic Retinopathy. PLOS ONE 7, e52699.

McCloskey, M., Wang, H., Jiang, Y., Smith, G.W., Strange, J., Hartnett, M.E., 2013. Anti-VEGF Antibody Leads to Later Atypical Intravitreous Neovascularization and Activation of Angiogenic Pathways in a Rat Model of Retinopathy of Prematurity. Invest. Ophthalmol. Vis. Sci. 54, 2020–2026.

Natoli, R., Valter, K., Barbosa, M., Dahlstrom, J., Rutar, M., Kent, A., Provis, J., 2013. 670nm Photobiomodulation as a Novel Protection against Retinopathy of Prematurity: Evidence from Oxygen Induced Retinopathy Models. PLOS ONE 8, e72135.

Nguyen, M.-T.T., Vemaraju, S., Nayak, G., Odaka, Y., Buhr, E.D., Alonzo, N., Tran, U., Batie, M., Upton, B.A., Darvas, M., Kozmik, Z., Rao, S., Hegde, R.S., Iuvone, P.M., Van Gelder, R.N., Lang, R.A., 2019. An opsin 5–dopamine pathway mediates light-dependent vascular development in the eye. Nature Cell Biology 21, 420–429.

Ota, W., Nakane, Y., Hattar, S., Yoshimura, T., 2018. Impaired Circadian Photoentrainment in Opn5-Null Mice. iScience 6, 299–305.

Owen, L.A., Morrison, M.A., Hoffman, R.O., Yoder, B.A., DeAngelis, M.M., 2017. Retinopathy of prematurity: A comprehensive risk analysis for prevention and prediction of disease. PLoS One 12.

Quinn, G.E., Ying, G.-S., Bell, E.F., Donohue, P.K., Morrison, D., Tomlinson, L.A., Binenbaum, G., G-ROP Study Group, 2018. Incidence and Early Course of Retinopathy of Prematurity: Secondary Analysis of the Postnatal Growth and Retinopathy of Prematurity (G-ROP) Study. JAMA Ophthalmol 136, 1383–1389.

Rao, S., Chun, C., Fan, J., Kofron, J.M., Yang, M.B., Hegde, R.S., Ferrara, N., Copenhagen, D.R., Lang, R.A., 2013. A direct and melanopsin-dependent fetal light response regulates mouse eye development. Nature 494, 243–246.

Rivera, J.C., Duchemin-Kermorvant, E., Dorfman, A., Zhou, T.E., Ospina, L.H., Chemtob, S., 2018. Retinopathy of Prematurity, in: Buonocore, G., Bracci, R., Weindling, M. (Eds.), Neonatology: A Practical Approach to Neonatal Diseases. Springer International Publishing, Cham, pp. 1–39.

Roohipoor, R., Karkhaneh, R., Riazi-Esfahani, M., Ghasemi, F., Nili-Ahmadabadi, M., 2009. Surgical Management in Advanced Stages of Retinopathy of Prematurity; Our Experience. J Ophthalmic Vis Res 4, 185–190.

Sapieha, P., Joyal, J.-S., Rivera, J.C., Kermorvant-Duchemin, E., Sennlaub, F., Hardy, P., Lachapelle, P., Chemtob, S., 2010. Retinopathy of prematurity: understanding ischemic retinal vasculopathies at an extreme of life. J Clin Invest 120, 3022–3032.

Scott, A., Fruttiger, M., 2010. Oxygen-induced retinopathy: a model for vascular pathology in the retina. Eye 24, 416–421.

Smith, L.E.H., 2003. Pathogenesis of retinopathy of prematurity. Seminars in Neonatology, Conundrums and Controversies in Neonatal Intensive Care 8, 469–473.

Smith, L.E.H., Wesolowski, E., McLellan, A., Kostyk, S.K., D'Amato, R., Sullivan, R., D'Amore, P.A., 1994. Oxygen-induced retinopathy in the mouse. Invest. Ophthalmol. Vis. Sci. 35, 101–111.

Stahl, A., Connor, K.M., Sapieha, P., Willett, K.L., Krah, N.M., Dennison, R.J., Chen, J., Guerin, K.I., Smith, L.E.H., 2009. Computer-aided quantification of retinal neovascularization. Angiogenesis 12, 297–301.

Terry, T.L., 1942. Fibroblastic Overgrowth of Persistent Tunica Vasculosa Lentis in Infants Born Prematurely. Trans Am Ophthalmol Soc 40, 262–284.

Wang, H., 2016. Anti-VEGF therapy in the management of retinopathy of prematurity: what we learn from representative animal models of oxygen-induced retinopathy [WWW Document]. Eye and Brain.

Xiao, S., Bucher, F., Wu, Y., Rokem, A., Lee, C.S., Marra, K.V., Fallon, R., Diaz-Aguilar, S., Aguilar, E., Friedlander, M., Lee, A.Y., 2017. Fully automated, deep learning segmentation of oxygen-induced retinopathy images. JCI Insight 2.

Yang, M.B., Rao, S., Copenhagen, D.R., Lang, R.A., 2013. Length of day during early gestation as a predictor of risk for severe retinopathy of prematurity. Ophthalmology 120, 2706–2713.